The theoretical investigation of $(CdTe)_{34}$ and Ag-doped $(CdTe)_{34}$ nanoclusters

Fengyi Suo[1], Yonghong Zhang[2]

[1,2] School of Science, Tianjin Polytechnic University, 300387, Tianjin, China

Abstract: Cadmium chalcogenide semiconductor, especially doped nanoclusters, have attracted so much concern for their tunability of its electronic properties. Here, the ultra-stable $(CdTe)_{34}$ core-cage and Ag-doped $(CdTe)_{34}$ core-cage structure have been investigated by density functional theory. Considering the effect of doping site in Ag-doped $(CdTe)_{34}$ nanocluster, three possible substitutional sites (S_1, S_2, S_3) are discussed. Based on it, the structural and electrical properties are studied in detail. Indeed, the Ag atom doping affect its original symmetry group and size. Particular attention is paid to the effects of Ag atom doping and substitutional sites. The results show that the Ag-doped $(CdTe)_{34}$ possess higher stability compared with undoped $(CdTe)_{34}$ nanocluster, and the stability varies with the different substitutional sites. Furthermore, the energy gap, density of states and charge density distributions have been analyzed, revealing that one new energy level called acceptor level is introduced in the original system. The charge distribution of acceptor level which is between valence band and conduction band, mainly from p-orbital of three Te atoms being around Ag atom and d-orbital of Ag atom. These illustrates metal(Ag atom) doping and substitutional sites are two important factors for its electrical properties.

Keywords: Cadmium telluride; Ag doping; Density functional theory; Structural and electrical properties.

1. INTRODUCTION

As one of typical Ⅱ-Ⅵ semiconductor materials, CdTe nanoclusters have attracted so much of physicists on account of their relevance in opto-electronic device. Due to the the effect of quantum confinement [1], the electrical properties of CdTe nanocluster sensitively depending on its size can be modified, which differs from bulk materials. Furthermore, tunability of the energy gap of these cluster by size or by impurity makes it extremely important for nano devices. Following these, different highly stable CdTe or CdSe quantum dots materials are synthesized to use for wide optoelectronic devices such as solar cells, infrared photo dection, light emitting diodes [2,5]. However, it is still difficult to clarify the relationship between the electrical properties with its the structure. To further elucidate the properties, a mass of structure were predicted and investigated [6,8] such as cage, core-cage and nanochains structure [9]. These researches show that the symmetry group transform, together with its stability and energy gap.

Doping is also one process which inevitably causes the altering of its properties because metal atoms are intentionally used to replace some atoms of the initial structure [10,12]. When one Cd atom was replaced in $(CdTe)_n$ nanoclusters, Pb/Ag-doped clusters were p-type semiconductors and In-doped clusters were n-type semiconductors. Furthermore, S. Xu et al. proved that the Ag doped ZnSe nanocrystals were more stable compared with the pure ZnSe [10]. In view of semiconductor nanolcusters, it is essential to investigate the structural and electronic properties of metal-doped semiconductor nanoclusters (NCs). However, for n>30, there is no publication which deals with the Ag-doped $(CdTe)_n$ nanoclusters.

In various nanoclusters, considering the $(CdSe)_{34}$ core-cage nanoclusters is one of ultra-stable nanoparticles [13], the stable $(CdTe)_{34}$ core-cage and Ag doped $(CdTe)_{34}$ core-cage structure are investigated. In this paper, the structure and electrical properties are studied by first-principles density functional theory (DFT). When one Cd atom is substituted by adjacent Ag atom, the initial cluster becomes a typical p-type NC. Due to the difference of substitutional sites, the properties change simultaneously. The structure and electronic properties are analyzed in detail, which include geometry, stability, the density of states, the electron density distributions of the highest occupied molecular orbital (HOMO) and lowest unoccupied molecular orbital (LUMO).

2. COMPUTATIONAL METHODS

The structure and electronic properties of $(CdTe)_{34}$ nanoclusters are calculated and studied by the well-known DFT [14,15]. In consideration of the disadvantage of Castep, the DMol^3 package [16] are implemented to compute and analyze in Materials Studio. The generalized-gradient approximation (GGA) with the Perdew, Burke and Ernzerhof correlation functionals (PBE) [17,18]. Furthermore, it is essential to choose the parameter standard, which causes the accuracy of the result. Four different accuracy can be chosen: coarse, medium, fine and customized respectively. In geometry optimization and property analysis, we choose the most accurate preferences.In the geometry optimization of $(CdTe)_{34}$ nanocluster, spin restriction and symmetry constraint need not to use. DNP basis is chosen to calculate and the self-consitency (SCF) cycles is 1000. Besides, the total energy convergence criterion is set as 10^{-6} Ha in SCF and the global orbital cutoff is 4.6 Å. Based on it, we calculate its frequency, fukui function and population analysis. To analyze the density of states (DOS) and band structure of $(CdTe)_{34}$ nanocluster, a large orthorhombic supercell is built to avoid their inter-cluster interaction. Here, $(CdTe)_{34}$ nanocluster is placed at the center of supercell. The distance from the surface $(CdTe)_{34}$ to the supercell boundary is more than 20 Å. On account of periodic boundary conditions, the DOS then can be analyzed. Next we substitute one Cd atom by the adjacent Ag atom in $(CdTe)_{34}$ nanoclusters. Compared with the initial structure, one electron is lost in $Cd_{33}Te_{34}Ag$ nanoclusters. In the geometry optimization, the spin-polarized calculations are adopted because one electron is lost compared to undoped clusters. Other parameters keep the same value with the undoped cluters.

3. RESULTS AND DISCUSSIONS

3.1 Structures of $(CdTe)_{34}$ and Ag-doped $(CdTe)_{34}$ nanoclusters

Considering the structure of $(CdSe)_{34}$ nanoclusters is ultra-stable [13], we investigate the $(CdTe)_{34}$ and Ag-doped $(CdTe)_{34}$ nanoclusters properties. The optimized structure are shown in Fig. 1. From the Fig. 1a, the stable $(CdSe)_{34}$ nanoclusters has a truncated-octahedral morphology formed by a $(CdTe)_{28}$ nanocluster and a $(CdTe)_6$ nanocluster encapsulated inside this cage. Here, the outside $(CdTe)_{28}$ cage is made up of 6 four-membered rings and 24 six-membered rings while the inside $(CdTe)_6$ cage contains 6 four-membered rings and 2 six-membered rings. Only Cd-Te bonds present in $(CdTe)_{34}$ nanoclusters. The Cd-Te bond length of $(CdTe)_{28}$ nanocluster is 2.88 Å while the $(CdTe)_6$ nanocluster bond length is 3.02 Å. The length of Cd-Te bond which interconnect the $(CdTe)_6$ and $(CdTe)_{28}$ nanocluster is 3.22 Å. This is caused by interatomic action force. Considering that doping can change the properties of NCs, one Cd atom is replaced by the adjacent Ag atom in $(CdTe)_{34}$ nanoclusters. Due to the difference of doping site, three possible substitutional sites are shown in Fig. 1. Thereinto, S_1 represents the outside Cd atom which shared by $(CdTe)_6$ and $(CdTe)_{28}$ nanocluster while S_2 represents the ouside Cd atom that not connect these two clusters. S_3 is the site which locates at $(CdTe)_6$ nanocluster. Due to it, the size of nanocluster changes simultaneously. From Table 1, the size of $Cd_{34}Te_{34}$ is 14.97 Å while the $Cd_{33}Te_{34}AgS_1$, $Cd_{33}Te_{34}AgS_2$ and $Cd_{33}Te_{34}AgS_3$ is 14.96 Å, 15.00 Å and 14.99 Å . This illustrates the Ag doping can change the size of $Cd_{34}Te_{34}$ cluster slightly. Also, the substitutional sites can affect it. Before doping, the symmetry group of $(CdTe)_{34}$ is C_3. And this symmetry loses when Ag atom doped in it.

Table I: The size L (Å), binding energy E_b (eV/cage) and HOMO-LUMO gap (eV) of $Cd_{34}Te_{34}$ and $Cd_{33}Te_{34}Ag$ nanoclusters.

Structure	L(Å)	E_b(eV/cage)	Gap(eV)
$Cd_{34}Te_{34}$	14.97	125.71	1.86
$Cd_{33}Te_{34}AgS_1$	14.96	126.40	1.82
$Cd_{33}Te_{34}AgS_2$	15.00	126.49	1.86
$Cd_{33}Te_{34}AgS_3$	14.99	126.92	1.88

3.2 The comparison of binding energy

To compare the stability of nanoclusters, we can calculate the its binding energy. The binding energy of $Cd_{34}Te_{34}$ cage is calculated by using the following equation:

$$E_b = [34 \times E(Cd) + 34 \times E(Te)] - E[(CdTe)_{34}]$$

Where $E(Cd)$, $E(Te)$ and $E((CdTe)_{34})$ represent the total energy of individual Cd, Te atoms and $(CdTe)_{34}$ cluster respectively. By calculation, the binding energy of $(CdTe)_{34}$ is 125.71 eV. After Ag doping, the binding energy equation becomes as follows:

$$E_b = [33 \times E(\text{Cd}) + 34 \times E(\text{Te}) + E(\text{Ag})] - E(\text{Cd}_{33}\text{Te}_{34}\text{Ag})$$

Similarly, the $E(\text{Cd})$, $E(\text{Te})$, $E(\text{Ag})$ and $E(\text{Cd}_{33}\text{Te}_{34}\text{Ag})$ is the total energy of individual Cd, Te, Ag and $\text{Cd}_{33}\text{Te}_{34}\text{Ag}$ cluster. From the Table 1, the $\text{Cd}_{33}\text{Te}_{34}\text{AgS}_1$, $\text{Cd}_{33}\text{Te}_{34}\text{AgS}_2$ and $\text{Cd}_{33}\text{Te}_{34}\text{AgS}_3$ is 126.40 eV, 126.49 eV and 126.92 eV. By comparison, the binding energy is large than the undoped $\text{Cd}_{34}\text{Te}_{34}$ cage. In other word, doping can improves the stability of $(\text{CdTe})_n$ nanoclusters, which keep the same conclusion with the former paper [10]. Furthermore, the binding energy is different when the substitutional site changes. The binding energy of $\text{Cd}_{33}\text{Te}_{34}\text{AgS}_3$ cluster is 0.52 eV and 0.43 eV higher than $\text{Cd}_{33}\text{Te}_{34}\text{AgS}_1$ and $\text{Cd}_{33}\text{Te}_{34}\text{AgS}_2$. This proves that the $\text{Cd}_{33}\text{Te}_{34}\text{AgS}_3$ cluster is more stable than the others. So we can replace one Cd atom being inside $(\text{CdTe})_6$ cluster to achieve more stable structure.

3.3 The comparison of energy gap

The differences of the highest occupied molecular orbital (HOMO) and the lowest unoccupied molecular orbital (LUMO) are listed in Table 1. From Table 1, the energy gap of $\text{Cd}_{33}\text{Te}_{34}\text{AgS}_N$ is 1.82 eV, 1.86 eV and 1.88 eV with N=1, 2, 3 respectively. The $\text{Cd}_{34}\text{Te}_{34}$ energy gap is 1.86 eV. The S_1 doping can narrow its initial gap while the S_3 doping enlarge its gap. S_2 doping do not change the original value. These results differs from the former conclusions [10]. Compared with $\text{Cd}_{33}\text{Te}_{34}\text{AgS}_2$ and $\text{Cd}_{33}\text{Te}_{34}\text{AgS}_3$, the less energy are need to excite electrons from their highest occupied valence band to their lowest unoccupied conduction band in $\text{Cd}_{33}\text{Te}_{34}\text{AgS}_1$ cluster. Thus it can be seen the substitutional doping can enlarge or keep the same of energy gap, not just narrow it.

3.4 The difference of DOS and PDOS

In order to further study the different orbital contribution to energy level, the total (TDOS) and partial density of states (PDOS) are figured in Fig.2, where the Fermi level is shifted to 0 eV and ploted in green dotted line. For the $(\text{CdTe})_{34}$, the energy band is observed to be divided into two parts: lower energy band with energy from -10.66 eV to 0.00 eV and higher unoccupied energy band with energy from 0.00 eV to 2.44 eV. After doping, considering one electron less as compared to the undoped system, the original cluster becomes typical p-type semiconductor. As a result, a hole is introduced in this system and the induced energy level is called acceptor level as shown in Fig. 2 E_a. The difference from the bottom of conduction band to the top of valence band is the energy gap. From Fig .2, the nature of HOMO and LOMO are not change too much when the Cd atom is replaced by the adjacent Ag atom, which is consistent with the above analysis. Furthermore, the E_a are near to the top of valence band, which illustrates Ag-doped $(\text{CdTe})_{34}$ is one of shallow acceptor doping. Compared with $\text{Cd}_{33}\text{Te}_{34}\text{Ag}_1$ and $\text{Cd}_{33}\text{Te}_{34}\text{Ag}_2$ nanoclusters, the E_a of $\text{Cd}_{33}\text{Te}_{34}\text{Ag}_3$ are closer to the Fermi level. To get the more shallow acceptor semiconductor, the substitutional site of Ag atom locates at the core $(\text{CdTe})_6$ in $(\text{CdTe})_{34}$ cluster.

The orbital contribution to different energy level are shown in Fig. 2 PDOS. For $(\text{CdTe})_{34}$ cluster, the strong s-orbital peaks are observed nearby the bottom of valence band (E=-11 eV). At the top of valence band (E=0 eV), the contribution of peaks mainly come from p-orbital along with minimal d-orbital. The peaks of the bottom of conduction band stem from p-orbital and partial d-orbital contribution. For $\text{Cd}_{33}\text{Te}_{34}\text{Ag}$ nanoclusters, the p-orbital and little d-orbital contribute to the E_a peak. In order to study the atomic orbital contributions of LUMO and HOMO, the charge density needs to be ploted.

3.5 The charge density distributions

Partial density of state of the $\text{Cd}_{33}\text{Te}_{34}\text{AgS}_1$ nanocluster are shown in Fig. 3. Here, LUMO represents the charge distribution of the bottom of conduction band while HOMO-2 is the top of valence band distribution in this nanocluster. HOMO is the electron density distribution of E_a (introduced Ag atom energy level). From Fig. 3a and 3b, the charge densities of LUMO mainly comes from p-orbital of Te atom and little hybrid d-orbital of Cd atom, without Ag atom contribution. The HOMO-2 charge density concludes p-orbital of Te atom and minor d-orbital of Ag atom, which proves the acceptor doping affect its distribution of conduction band. Form Fig. 3c and 3d, the acceptor level which is between valence band and conduction band, is observed mainly from p-orbital of three Te atoms being around Ag atom and d-orbital of Ag atoms. These keep the same conclusions with former study in Fig. 2.

4. CONCLUSIONS

In this paper, the structural and electronic properties of $(\text{CdTe})_{34}$ and $\text{Cd}_{33}\text{Te}_{34}\text{Ag}$ nanoclusters are calculated and investigated by density functional theory (DFT). Considering that doping can change the properties of NCs, three possible substitutional sites are discussed in detail. The results show that doping affect its original symmetry group and size.

Further stability study demonstrate that Ag-doping can make $(CdTe)_{34}$ nanocluster more stable. Also, different substitutional doping sites of Ag atom affect its stability. Compared with $Cd_{33}Te_{34}AgS_2$ and $Cd_{33}Te_{34}AgS_3$, the less energy are need to excite electrons from their highest occupied valence band to their lowest unoccupied conduction band in $Cd_{33}Te_{34}AgS_1$ cluster. The analyses of DOS and PDOS show that Ag-doped $(CdTe)_{34}$ is one of shallow acceptor doping. The original cluster becomes typical p-type semiconductor with a hole is introduced in this system. The contribution of induced energy level E_a (acceptor level) comes from the p-orbital of three Te atoms being around Ag atom and minor d-orbital of Ag atom. By analyzing the partial density of state, we knows that the E_a (acceptor level) charge distribution mainly from p-orbital of three Te atoms being around Ag atom and d-orbital of Ag atoms.

REFERENCES

[1] S.K. Haram et al., "Quantum Confinement in CdTe Quanturn Dots: Investigation through Cyclic Voltammetry Supported by Density Functional Theory (DFT)," J.Phys. Chem. C, 115, 6243–6249. 2011.

[2] G.H. Ahmed et al., "The impact of electrostatic interactions on ultrafast charge transfer at Ag_{29} nanoclusters-fullerene and CdTe quantum dots-fullerene interfaces," J. Mater. Chem. C, 4, 2894-2900. 2016.

[3] X. Shen, J. Jia, Y. Lin, X. Zhou, "Enhanced performance of CdTe quantum dot sensitized solar cell via anion exchanges," J. Power Sources, 277,215-221.2015.

[4] A.D. Stiff-Roberts, K.R. Lantz, R. Pate, "Room-temperature, mid-infrared photodetection in colloidal quantum dot/conjugated polymer hybrid nanocomposites: a new approach to quantum dot infrared photodetectors," J. Phys. D: Appl. Phys, 42, 234004. 2009.

[5] S. Dolai et al., "Mechanistic study of the formation of bright white light-emitting ultrasmall CdSe nanocrystals: role of phosphine free selenium precursors," Chem. Mater, 10, 1021, 2015

[6] S. Sriram and R. Chandiramouli, "DFT studies on the stability of linear, ring, and 3D structures in CdTe nanoclusters," Res. Chem. Intermed, 41,2095–2124. 2015.

[7] S.K.Bhattacharya and A. Kshirsagar, "Ab initio calculations of structural and electronic properties of CdTe clusters," Phys. Rev. B, 75, 035402. 2007.

[8] L. Ma and J. Wang, G. Wang, "Search for global minimum geometries of medium sized Cd_nTe_n clusters (n=15, 16, 20, 24 and 28)," Chem. Phys, Lett, 552, 73-77. 2012.

[9] Z. Wu, Y. Zhang, S. Huang and S. Zhang, "Theoretical inverstigation of assembled $(CdTe)_{12\times N}$ (N=1－5) multi-cage nanochains," Comput. Mater. Sci, 68, 238-244. 2013.

[10] S. Xu et al., "Theoretical and experimental investigation of stability and spectra of doped Ag:ZnSe nanocrystals," J. Mol. Model, 20,2184. 2014.

[11] Z. Rak, S.D.Mahanti, K.C. Mandal and N.C. Fernelius, "Electronic structure of substitutional defects and vacancies in GaSe," J. Phys. Chem. Solids, 70, 344–355. 2009.

[12] S.K.Bhattacharya and A. Kshirsagar, "Defect studies in small CdTe clusters," Eur. Phys. J. D, 61, 609–619. 2011.

[13] A. Kasuya et al., "Ultra-stable nanoparticles of CdSe revealed from mass specteometry," Nature Mater, 10,1038. 2004.

[14] R. Car and M. Parrinello, "Unified Approach for Molecular Dynamics and Density-Functional Theory," Phys. Rev. Lett, 55, 2471.

[15] R. O. Jones, Rev and Mod, "Density functional theory: Its origins, rise to prominence, and future," Phys, 87, 897.

[16] B. Delley, "From molecules to solids with the $DMol^3$ approach," J. Chem. Phys, 7756-7764. 2000.

[17] J.P. Perdew, K. Burke and Y. Wang, "Generalized gradient approximation for the exchange-correlation hole of a many-electron system," Phys. Rev. B, 54, 16533.

[18] B.Hammer, L. B. Hansen and J. K. Norskov, "Improved adsorption energetics within density-functional theory using revised Perdew-Burke-Ernzerhof functionals," Phys. Rev. B, 59, 7413.
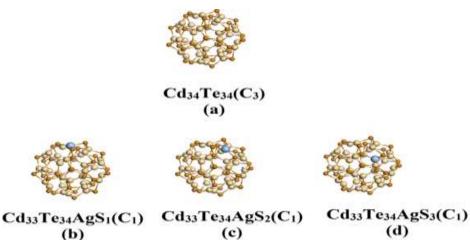
APPENDIX – A

LIST OF FIGURES:

Fig. 1. The geometry structures of Cd$_{34}$Te$_{34}$ and Cd$_{33}$Te$_{34}$Ag nanoclusters. Blue bigger balls represent Ag atoms, light brown middle balls represent Cd atoms and dark brown small balls represent Te atoms.
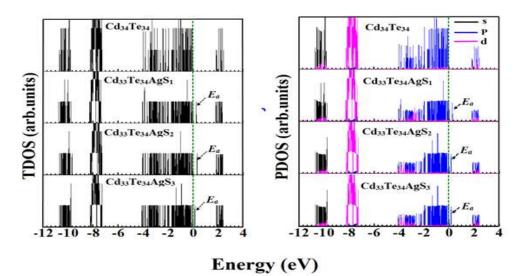

Fig. 2. The total (TDOS) and partial density of state (PDOS) of Cd$_{34}$Te$_{34}$ and Cd$_{33}$Te$_{34}$Ag nanoclusters. Here, the Fermi level is shifted to 0 eV.
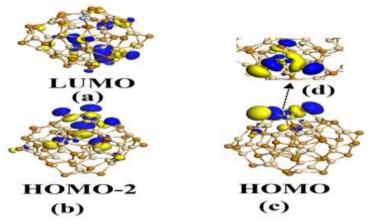

Fig. 3. Partial density of state of the Cd$_{33}$Te$_{34}$AgS$_1$ nanocluster, (a) LUMO, (b) HOMO-2, (c) HOMO, (d) enlarged view of the HOMO-2.